JOURNAL OF SYNCHROTRON RADIATION

ISSN 1600-5775

3D imaging of a rice pollen grain using transmission X-ray microscopy

Shengxiang Wang,[a] Dajiang Wang,[a] Qiao Wu,[b] Kun Gao,[a] Zhili Wang[a]* and Ziyu Wu[c]†

[a]National Synchrotron Radiation Laboratory, University of Science and Technology of China, 42 Hezuohua South Road, Hefei, Anhui 230029, People's Republic of China, [b]Department of Biochemistry, School of Life Sciences, Fudan University, Shanghai 200433, People's Republic of China, and [c]Institute of High Energy Physics, Chinese Academy of Sciences, Beijing 100049, People's Republic of China.
*Correspondence e-mail: wangnsrl@ustc.edu.cn

Received 12 February 2015
Accepted 20 May 2015

Edited by P. A. Pianetta, SLAC National Accelerator Laboratory, USA

† Deceased.

Keywords: transmission X-ray microscopy; nano-tomography; rice pollen grain; cellular microstructure.

For the first time, the three-dimensional (3D) ultrastructure of an intact rice pollen cell has been obtained using a full-field transmission hard X-ray microscope operated in Zernike phase contrast mode. After reconstruction and segmentation from a series of projection images, complete 3D structural information of a 35 μm rice pollen grain is presented at a resolution of ~100 nm. The reconstruction allows a clear differentiation of various subcellular structures within the rice pollen grain, including aperture, lipid body, mitochondrion, nucleus and vacuole. Furthermore, quantitative information was obtained about the distribution of cytoplasmic organelles and the volume percentage of each kind of organelle. These results demonstrate that transmission X-ray microscopy can be quite powerful for non-destructive investigation of 3D structures of whole eukaryotic cells.

1. Introduction

Rice (*Oryza sativa*) is one of the world's most consumed staple foods. Manipulation of pollen fertility is particularly important to fulfill the increasing demand of rice grain yield. Pollen is an important element of reproduction and evolution, and therefore pollen research is of great significance. Actually, what we need to know first is the morphology and structure of the pollen. Many different imaging techniques have been used to study both the structure and morphology of different kinds of pollen grains. However, those techniques have limitations in achieving high spatial resolution in the imaging of a whole pollen grain. In the case of optical microscopy, the spatial resolution is limited by the wavelength of visible light. Another widely used instrument is the electron microscope (EM). Research on different species of pollen has been reported since the introduction of the EM (Ehrlich, 1958; Skvarla & Larson, 1965). Although the spatial resolution of the EM can be down to several nanometers, it cannot obtain a real three-dimensional (3D) structure. Serial sectioning and acquisition of an entire set of images is required to cover an entire cell, but mechanical cutting generates the loss of sections and/or serious damage to the ultrastructure of pollen grains.

As an emerging imaging technique, transmission X-ray microscopy bridges the resolution gap between optical and electron microscopy. The combination of short wavelength and high penetrating power leads to the possibility of providing high-resolution images and 3D tomography without cutting sections of the sample. Regarding imaging research,

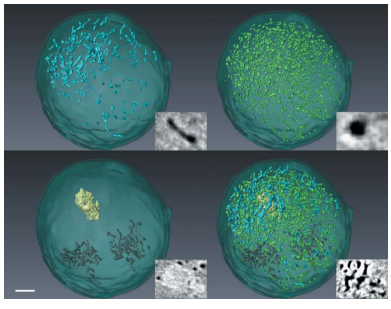

the use of X-rays can be divided into two categories: soft and hard X-ray microscopy. The occurrence of specific elemental absorption lines shows that organic materials exhibit a greater attenuation than water (Attwood, 1999). This region of the X-ray spectrum belongs to soft X-rays, which is usually recognized as the 'water window' region. There have been many important findings working with water window soft X-ray microscopes: the visualization of the whole cellular structure, hydrated cells (Magowan *et al.*, 1997; Methe *et al.*, 1997; Jacobsen, 1999) and tomography of various eukaryotic cells (Le Gros, 2005; Schneider *et al.*, 2010; Hummel *et al.*, 2012; Müller *et al.*, 2012) without staining. However, the depth of focus of soft X-ray microscopy is limited to several micrometers, which means that it is difficult to collect images of most eukaryotic cells with typical dimensions larger than 10 µm. In contrast, transmission hard X-ray microscopy can provide internal 3D structures of cells with a thickness up to 50 µm (Andrews *et al.*, 2010; Zhang *et al.*, 2013). This dimension already covers the size of most eukaryotic cells. Recently, there has been rapid developments in the construction and application of hard X-ray microscopes (Stampanoni *et al.*, 2010; Martinez-Criado *et al.*, 2012; Chen-Wiegart *et al.*, 2013).

In this contribution, we present 3D tomography of rice pollen grains using hard X-ray nano-tomography. Zernike phase contrast and heavy metal staining (Zheng *et al.*, 2012; Wang *et al.*, 2014) have been utilized to achieve high-quality tomography. The reconstructions clearly reveal subcellular structures within an intact cell. 3D segmentation provides the size and shape of the subcellular structures. Quantitative information, including the ratios of organelle volume over cell volume and the surface area to volume, have also been estimated.

2. Materials and methods

2.1. Sample preparation

Rice pollen grains were kept in the rice anther before being removed to perform X-ray imaging experiments. A small aperture was made in the top of the palea of each rice flower and the flower was soaked in 4.0% glutaraldehyde for 4 h at 277 K, then rinsed in a phosphate buffer solution (PBS) three times and post-fixed with 2% osmium tetroxide for 1 h at 277 K. After being rinsed three times with PBS, the flowers were stained with 2% uranyl acetate overnight to make sure they were fully stained and rinsed. Then they were stained with 2% lead citrate for 2 h. Finally, the flowers were rinsed and dehydrated in graded ethanol series of 50–100% and dried in air. The staining technique used here followed a similar approach to that found to be successful for electron microscope imaging of pollen (Echlin, 1965).

2.2. Transmission X-ray microscope

The nano-tomography experiments were performed using the transmission hard X-ray microscope (TXM) commissioned at beamline 4W1A of the Beijing Synchrotron Radiation Facility. An elliptically shaped capillary condenser was used to focus the incident X-rays onto the sample, and a phase ring was placed in the back focal plane of the objective to provide the Zernike phase contrast. A zone-plate objective magnified the sample images, which were finally recorded by a 1024 × 1024 charge coupled device camera. In our experiment, a layout with a large field of view was used: the field of view was 60 µm × 60 µm, the photon energy was 8 keV and the outermost zone width of the zone plate was 35 nm (Yuan *et al.*, 2012).

As mentioned above, in order to improve the image contrast of cell organelles, samples were stained with heavy metals and the TXM was operated in the Zernike phase contrast mode in an effort to further enhance the edge contrast of the organelles. Before setting the sample inside the TXM, some gold particles were carefully pasted on top of the sample using an optical microscope. These particles were used for alignment of serial tilts and for the tomographic reconstruction. A series of sequential projection images were recorded from −90° to +90° with 0.5° increment and an exposure time of 15 s for each projection. Projection data were reconstructed using a commercial software package provided by Xradia (Tkachuk *et al.*, 2007) while the segmentation was performed using *Avizo Fire 7.1* software (Visualization Sciences Group, Bordeaux, France).

3. Results and discussion

Pollen is considered to be an excellent model system for the study of meiotic events, cellular organization, cell–cell interactions and polar growth in plant biology (Bedinger *et al.*, 1994). It is not a simple cell and shows complex changes during the process of maturity. After analysis using the TXM, we then observed the structure using a scanning electron microscope (SEM) as contrast. As shown in Fig. 1(*a*), the extine, intine and some organelles of the rice pollen can be clearly recognized. They can also be recognized in the slice produced by the TXM (Fig. 1*b*). However, the TXM collects almost 1000 slices, which contain all the information required to form a 3D picture of the whole pollen grain, while the SEM only provides a random section. In other words, we can obtain more useful information from a TXM quickly. TXM slices were obtained from a rough 3D tomography directly generated by tilted serial projection

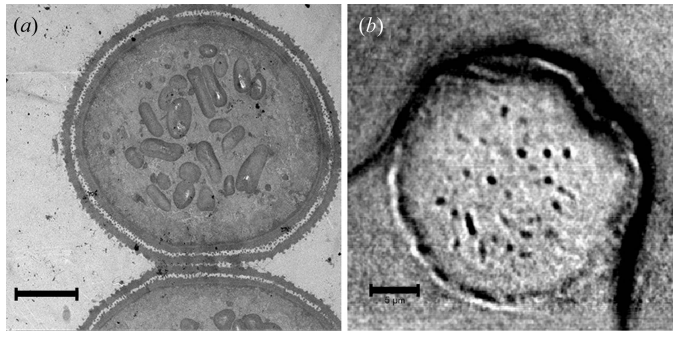

Figure 1
Rice pollen grain imaged by SEM (*a*) and TXM (*b*). Scale bars = 5 µm.

drawings using a standard filtered back-projection algorithm (Kak & Slaney, 1988).

We stained the sample to improve the absorption contrast and used a phase ring to increase the phase contrast. Intrinsic characteristics of organelles, such as linear absorption coefficient, size and shape, help to distinguish different organelles within the rice pollen (Parkinson *et al.*, 2008). Moreover, the Zernike phase contrast provides a good differentiation of the organelles. Due to the 'hole effect' produced by the phase contrast (Youn & Jung, 2006), bright boundaries surrounding the organelles are more obvious. According to the clear boundaries of the cytoplasmic organelles and the cell wall of rice pollen in each reconstructed slice, a 3D segmentation and rendering of the rice pollen was performed. Images showing four colors of organelles based on this procedure can be seen in Fig. 2.

Through the use of segmentation and rendering, the size, shape and distribution of the pollen organelles are presented in Fig. 2. The largest number of organelles, marked in green, also having a low grey-value, are lipid bodies (Fig. 2*b*). The cylindrical material marked in blue are mitochondria, and the distribution shows that the mitochondria tend to be on one side of the cell. The yellow material is the vacuole, with the highest grey-value. The black material in the 3D tomography corresponds to the nuclei, which are under caryomitosis and react in the inner edge of the cell, particularly on the maturing process of the pollen grain (Fig. 2*c*). Detailed microstructural parameters obtained from the segmentation process are listed in Table 1. The volume and superficial area of the rice pollen grain are 2968.3 μm^3 and 7833.7 μm^2, respectively. Among all the organelles, the lipid body occupies the highest volume percentage, *i.e.* 9.98%. This means that the lipid body plays an important role in the growth of the pollen. Mitochondria and vacuole occupy 2.37% and 3.54% of the pollen volume, respectively, and the volume of the nucleus is about 2.25% of the entire cellular volume. Note that the volume content of each kind of organelle is low while the ratio of surface area to volume is always high. This results in a large effective contact area to the cytoplasm, which is meaningful to the organelles for it helps improve the material exchange efficiency.

Table 1
Microstructural parameters of the organelles in the rice pollen grain.

	Volume (μm^3)	Area (μm^2)	Surface area to volume ratio (μm^{-1})	Volume fraction
Vacuole	105.0	297.4	2.83	3.54%
Nucleus	66.9	384.4	5.75	2.25%
Lipid body	296.2	3373.4	11.39	9.98%
Mitochondrion	70.3	565.4	8.05	2.37%
Pollen	2968.3	7833.7	2.64	

Pollen grains are embedded in a resistant wall, in order to permit the pollen tube germination. They have a structure called the aperture, where the pollen wall is reduced or absent. It is usually located at the distal pole. From the reconstruction we obtain slices of the pollen aperture. The extine, intine and the location of the aperture (red arrow) can be clearly distinguished from the virtual cross-section [Figs. 3(*a*) and 3(*b*)]. As shown in the 3D rendering, the thickness of the wall is about 1 μm and a prospective germination site can be easily observed [Figs. 3(*c*) and 3(*d*)]. Rice belongs to the monocot family and usually has only one aperture, so the development of this aperture is important for fertilization. During the long period of pollen maturation, its cytoplasm undergoes massive structural and metabolic changes. Different from seeds where proteins are the most important reserves, carbohydrates and lipids are the principal reserves in mature pollen (Pacini, 1996). Data shown in Table 1 confirm this claim. We also find that lipid bodies and mitochondria, which gathered on the side of the aperture, are ready for the germination of the pollen grain (Fig. 3*d*). Polarization of lipid bodies towards the aperture could also prevent water loss.

The major advantage of the TXM technique is that it can obtain 3D structural information of the cell in a near natural state. This unique capability makes it an ideal tool for cellular imaging research. Different

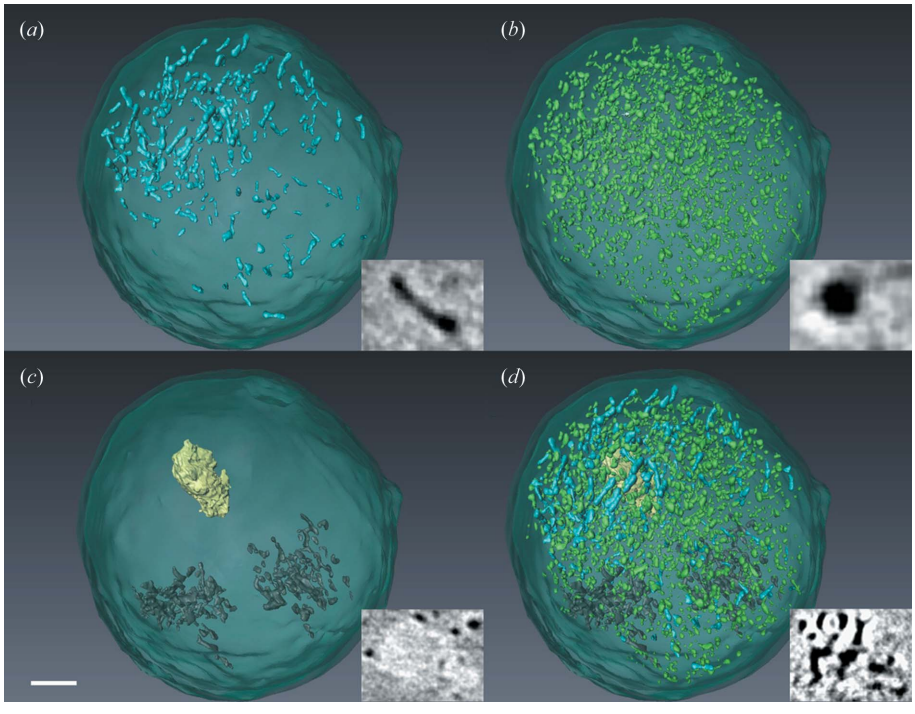

Figure 2
3D rendering of rice pollen. (*a*) Cell wall marked in cyan and mitochondrion marked in blue. (*b*) Lipid body marked in green. (*c*) Vacuole marked in yellow and nuclei marked in black. (*d*) Complete view of the whole rice pollen. The lower right-hand corner of each image shows a two-dimensional slice of mitochondrion, lipid body, vacuole and nucleus, respectively. Scale bar = 5 μm.

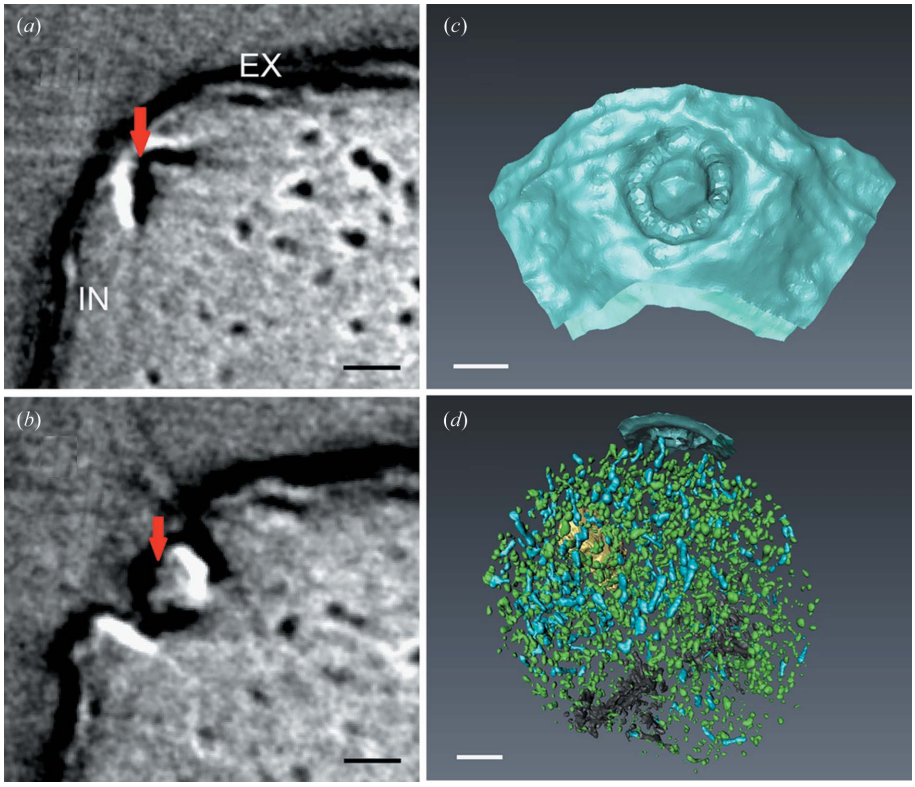

Figure 3
Pollen aperture imaged by hard X-ray microscopy. (*a*), (*b*) 2D virtual cross-sections of the rice pollen aperture from TXM reconstruction. Scale bar = 2.5 µm. (*c*) 3D rendering of the pollen aperture. Scale bar = 2 µm. (*d*) 3D rendering of the whole cell with the transparent cell wall and shaded pollen aperture. Scale bar = 5 µm.

varieties of rice pollens may have a different percentage composition of the cytoplasmic organelles. For example, genetically modified rice can significantly increase the yield of rice *via* gene expression, which can change both the quantity and the volume of some organelles. From a 3D tomography achieved using a TXM, we can easily locate those organelles and obtain their structural parameters. It is also a helpful tool for transgenosis engineering research.

However, some structures cannot be detected in TXM images. A possible reason for this is that some organelles are not stained with the technique that we used. Another reason is that the dimensions of the organelles fall below the current resolution of the TXM. The foreseen development in the manufacture of optical elements and staining technology will certainly improve the performance of TXMs and this instrument will certainly play an important role in biological science.

4. Conclusion

In this study we demonstrated that transmission hard X-ray microscopy is suitable for morphology research of eukaryocytes. We provided 3D substructure tomography of rice pollens and the volume percentage of their cytoplasmic organelles. The distribution of organelles also reveals some of the roles they play. Data and images clearly confirm that TXM is a perfect tool for revealing secrets of the development, evolution and variation of many species. It may offer precious information capable of guiding the evolution and the variation in many different directions.

Acknowledgements

We would like to thank Huang Wei from Fudan University for providing rice pollen and for many suggestions on how to distinguish the organelle of rice pollen. This work has been supported by the National Basic Research Program of China (2012CB825801), the National Natural Science Foundation of China (11205157, 11475170) and the Anhui Provincial Natural Science Foundation (1508085MA20).

References

Andrews, J. C., Almeida, E., van der Meulen, M. C., Alwood, J. S., Lee, C., Liu, Y., Chen, J., Meirer, F., Feser, F., Gelb, J., Rudati, J., Tkachuk, A., Yun, W. & Pianetta, P. (2010). *Microsc. Microanal.* **16**, 327–336.
Attwood, D. (1999). *Soft X-rays and Extreme Ultraviolet Radiation: Principles and Applications.* Cambridge University Press.
Bedinger, P. A., Hardeman, K. J. & Loukides, C. A. (1994). *Trends Cell Biol.* **4**, 132–138.
Chen-Wiegart, Y. K., Liu, Z., Faber, K. T., Barnett, S. A. & Wang, J. (2013). *Electrochem. Commun.* **28**, 127–130.
Echlin, P. (1965). *J. Cell Biol.* **24**, 150–153.
Ehrlich, H. G. (1958). *Exp. Cell Res.* **15**, 463–474.
Hummel, E., Guttmann, P., Werner, S., Tarek, B., Schneider, G., Kunz, M., Frangakis, A. S. & Westermann, B. (2012). *PloS One*, **7**, e53293.
Jacobsen, C. (1999). *Trends Cell Biol.* **9**, 44–47.
Kak, A. C. & Slaney, M. (1988). *Principles of Computerized Tomographic Imaging*, IEEE Service Centre, Piscataway, New Jersey, USA.
Le Gros, M. A., McDermott, G. & Larabell, C. A. (2005). *Curr. Opin. Struct. Biol.* **15**, 593–600.
Magowan, C., Brown, J. T., Liang, J., Heck, J., Coppel, R. L., Mohandas, N. & Meyer-Ilse, W. (1997). *Proc. Natl Acad. Sci. USA*, **94**, 6222–6227.
Martínez-Criado, G., Tucoulou, R., Cloetens, P., Bleuet, P., Bohic, S., Cauzid, J., Kieffer, I., Kosior, E., Labouré, S., Petitgirard, S., Rack, A., Sans, J. A., Segura-Ruiz, J., Suhonen, H., Susini, J. & Villanova, J. (2012). *J. Synchrotron Rad.* **19**, 10–18.
Methe, O., Spring, H., Guttmann, P., Schneider, G., Rudolph, D., Trendelenburg, M. F. & Schmahl, G. (1997). *J. Microsc.* **188**, 125–135.
Müller, W. G., Bernard Heymann, J., Nagashima, K., Guttmann, P., Werner, S., Rehbein, S., Schneider, G. & McNally, J. G. (2012). *J. Struct. Biol.* **177**, 179–192.
Pacini, E. (1996). *Sex. Plant Reprod.* **9**, 362–366.
Parkinson, D. Y., McDermott, G., Etkin, L. D., Le Gros, M. A. & Larabell, C. A. (2008). *J. Struct. Biol.* **162**, 380–386.
Schneider, G., Guttmann, P., Heim, S., Rehbein, S., Mueller, F., Nagashima, K., Heymann, J. B., Müller, W. G. & McNally, J. G. (2010). *Nat. Methods*, **7**, 985–987.
Skvarla, J. J. & Larson, D. A. (1965). *Grana*, **6**, 210–269.

Stampanoni, M., Mokso, R., Marone, F., Vila-Comamala, J., Gorelick, S., Trtik, P., Jefimovs, K. & David, C. (2010). *Phys. Rev. B*, **81**, 140105.
Tkachuk, A., Duewer, F., Cui, H., Feser, M., Wang, S. & Yun, W. (2007). *Z. Kristallogr.* **222**, 650–655.
Wang, D., Li, N., Wang, Z., Gao, K., Zhang, Y., Luo, Y., Wang, S., Bao, Y., Shao, Q. & Wu, Z. (2014). *J. Synchrotron Rad.* **21**, 1175–1179.
Youn, H. S. & Jung, S. W. (2006). *J. Microsc.* **223**, 53–56.
Yuan, Q., Zhang, K., Hong, Y., Huang, W., Gao, K., Wang, Z., Zhu, P., Gelb, J., Tkachuk, A., Hornberger, B., Feser, M., Yun, W. & Wu, Z. (2012). *J. Synchrotron Rad.* **19**, 1021–1028.
Zhang, K., Li, D. E., Hong, Y. L., Zhu, P. P., Yuan, Q. X., Huang, W. X., Gao, K., Zhou, H. Z. & Wu, Z. Y. (2013). *Chinese Phys. B*, **22**, 076801.
Zheng, T., Li, W., Guan, Y., Song, X., Xiong, Y., Liu, G. & Tian, Y. (2012). *Microsc. Res. Tech.* **75**, 662–666.